HHS Public Access

Author manuscript

Virology. Author manuscript; available in PMC 2017 January 01.

Published in final edited form as:

Virology. 2016 January ; 487: 249–259. doi:10.1016/j.virol.2015.10.019.

Combined Therapy of Oncolytic Adenovirus and Temozolomide Enhances Lung Cancer Virotherapy *In Vitro* and *In Vivo*

Jorge G. Gomez-Gutierrez[a,c,*], **Jonathan Nitz**[a], **Rajesh Sharma**[b,c], **Stephen L. Wechman**[a], **Eric Riedinger**[a], **Elvis Martinez-Jaramillo**[a], **Heshan Sam Zhou**[a,c], and **Kelly M. McMasters**[a,c]

[a] The Hiram C. Polk Jr, MD, Department of Surgery, University of Louisville School of Medicine, Louisville, KY, 40202, USA.

[b] Department of Medicine, University of Louisville School of Medicine, Louisville, KY, 40202, USA.

[c] James Graham Brown Cancer Center, University of Louisville School of Medicine, Louisville, KY, 40202, USA.

Abstract

Oncolytic adenoviruses (OAds) are very promising for the treatment of lung cancer. However, OAd-based monotherapeutics have not been effective during clinical trials. Therefore, the effectiveness of virotherapy must be enhanced by combining OAds with other therapies. In this study, the therapeutic potential of OAd in combination with temozolomide (TMZ) was evaluated in lung cancer cells *in vitro* and *in vivo*. The combination of OAd and TMZ therapy synergistically enhanced cancer cell death; this enhanced cancer cell death may be explained via three related mechanisms: apoptosis, virus replication, and autophagy. Autophagy inhibition partially protected cancer cells from this combined therapy. This combination significantly suppressed the growth of subcutaneous H441 lung cancer xenograft tumors in athymic nude mice. In this study, we have provided an experimental rationale to test OAds in combination with TMZ in a lung cancer clinical trial.

Keywords

Lung; Cancer; Oncolytic; Adenovirus; Temozolomide; Autophagy; Apoptosis

Introduction

Lung cancer remains the leading cause of death from cancer worldwide (Murray and Lopez, 2013). Most chemotherapy and molecular therapies are based on the induction of apoptosis. However, tumors frequently develop resistance to apoptosis prior to or during cancer

[*]Corresponding author: Jorge G. Gomez-Gutierrez, 505 South Hancock, Kosair Charities Clinical & Translational Research (KCCTR) Building, Room 452G, Louisville, KY, 40202, USA. Tel.: (502)-852-8464; Fax: (502)-852-3661; jgguti01@louisville.edu.

treatment (Zhang et al., 2006). Temozolomide (TMZ), an alkylating agent in monotherapy or in association with irinotecan, has been tested as a second- (or third-) line therapy in patients with non-small cell lung carcinoma (NSCLC). TMZ is, however, associated with low response rates (Tatar et al., 2013), which may be due to increased expression of the DNA repair enzyme, O6-methylguanine-DNA methyltransferase (MGMT), in NSCLC tumors (Mattern et al., 1998).

One very promising approach for the treatment of lung cancer tumors is the use of oncolytic adenoviruses (OAds). OAds-based monotherapeutic clinical trials, however, have not met expectations. Therefore, the effectiveness of oncolytic virotherapy must be enhanced with the combination of other therapies (*i.e.*, chemotherapy or immunotherapy).

The combination of oncolytic adenoviruses and TMZ significantly enhanced the melanoma and glioblastoma antitumor response *in vitro* and *in vivo* (Jiang et al., 2015); (Kaliberova et al., 2009). This enhanced antitumor response was due to autophagy induction by TMZ (Tyler et al., 2009; Ulasov et al., 2009a). Autophagy involves the degradation of unnecessary or dysfunctional cellular components. The breakdown of cellular components can ensure cellular survival during starvation and stress by maintaining cellular energy levels (Newman et al., 2007). Autophagy has a dual role, acting as a survival mechanism and as a caspase-independent form of programmed cell death (Gozuacik and Kimchi, 2007).

There are two types of lung cancer cells in terms of OAds replication efficiency: permissive or semi-permissive. Oncolytic Ad replication is greater in permissive cancer cells than in semi-permissive cancer cells (Hay et al., 1999). Therefore, to improve the therapeutic efficacy of OAds to treat heterogeneous NSCLC tumors, OAds replication must be enhanced in both permissive and semi-permissive lung cancer cells. In this study, we investigated whether TMZ-induced autophagy could enhance virotherapy in both permissive and semi-permissive lung cancer cells. The combination of OAd and TMZ therapy was highly effective *in vitro* and *in vivo*.

Results

Evaluation of virotherapy and chemotherapy killing effect on permissive and semi-permissive lung cancer cells

Multiple lung cancer cell lines were infected with the following two adenoviruses: adenovirus serotype 5 wild type (Adwt) and E1B-deleted Adhz60 (Adhz60). At 72 h post-infection, crystal violet staining revealed that cytopathic effects (CPE) increased in a virus dose-dependent manner (Fig 1A). Sensitivity to Adwt and Adhz60 was variable across these cancer cell lines. Furthermore, the estimated half maximal inhibitory concentration (IC_{50}) of Adwt ranged from a multiplicity of infection (MOI) concentration of 1 to 10, depending upon the cancer cell line. Adhz60 efficiently induced CPE in H1299 and A549 cells at low MOI concentrations (1 and ~ 3, respectively) (Fig. 1A). In contrast, the semi-permissive Calu1 and H441 cells showed greater resistance to CPE induced by both Adwt and Adhz60. Adhz60 IC_{50} for Calu-1 cells was reached at an 10 MOI, whereas the IC_{50} was approximately reached at 20 MOI for H441 cells (Fig. 1B). Adwt could induce IC_{50} in Calu-1 and H441 cells, but at greater rates of MOI (5 and 10, respectively) in comparison

with permissive cancer cells, in which IC_{50} was a rate less than 1 MOI (Fig. 1B). Next, the TMZ IC_{50} was determined. Lung cancer cell lines were treated at increasing TMZ concentrations. At 72 h post-treatment, an MTT assay revealed that cell viability inhibition increased in a dose-dependent manner with increasing TMZ concentration. Sensitivity to TMZ was also variable across cancer cell lines. Calu-1 showed greater resistance to TMZ. The IC_{50} of TMZ in H441 and A549 cells was at 1 and 0.75 mM, respectively. In Calu1 and H1299, the IC_{50} of TMZ was not reached under this experimental condition (Fig. 1C).

The combined therapy of Adhz60 with TMZ resulted in a synergistic lung cancer killing effect

The effect of the combination of Adhz60 and TMZ upon cell viability was analyzed for synergy. Adhz60 at 1 MOI efficiently destroyed H1299 cells as shown in Figure 1A; therefore, H1299 cells were removed from further experimentation.

Lung cancer cell lines were infected with Adhz60 at their respective IC_{50} doses in combination with their respective TMZ IC_{50} doses. DMSO was added at its respective volume as control. At 72 h post-treatment, crystal violet staining results showed that the combination of Adhz60 and TMZ (Adhz60 + TMZ) induced greater cytotoxicity in all three cancer cell lines treated than in the oncolytic virus or TMZ treatments alone (Fig. 1D) (Supplementary 1). We then evaluated these quantitated data by fraction affected versus combination index (Fa-Cl) with CalcuSyn software to assess if this interaction between TMZ and Adhz60 was synergistic or not (Biosoft, Ferguson, MO) (Fig. 1E). The cell viability was significantly lower with the combination of Adhz60 + TMZ than with Adhz60 alone, TMZ alone, with replication-incompetent AdLacZ expressing β-galactosidase + TMZ, or with controls (mock + Ad-LacZ) (Fig. 1D). The middle curve line represents the simulated combination index values of the combination treatment groups surrounded by two lines of algebraic estimations of the 95% Confidence Intervals. Most of the experimental CI values at the tested ratio were < 1 and between the two Confidence lines, indicating synergism of combination treatments ($p < 0.05$) (Fig. 1E). These results indicate that the combination therapy (Adhz60 + TMZ) resulted in synergistic cytotoxicity in multiple human lung cancer cell lines.

The synergistic killing effect of combined therapy using oncolytic adenovirus and TMZ was, in part, due to apoptosis

The activation of caspase-3 was evaluated next. Immunoblot analysis revealed greater expression of cleaved caspase-3 in cells treated with Adhz60 + TMZ than in either treatment alone (Fig. 2A). Additionally, annexin V staining also showed a greater proportion of apoptotic cells when treated with the combination of both Adhz60 and TMZ than in either treatment alone (Fig 2B). In A549 cells, Adhz60 and TMZ induced 14% and 26% of apoptosis, respectively, whereas the combined therapy resulted in 60% of apoptosis (Fig. 2C). In H441 cells, Adhz60 and TMZ induced 13% and 14% of apoptosis, respectively, whereas the combination therapy resulted in a 30% of apoptosis (Fig. 2C). In Calu1 cells, Adhz60 and TMZ induced 10% and 13% apoptosis, respectively, whereas the combination of both induced 32% apoptosis (Fig. 2C). These results suggest that the synergistic killing

effect of lung cancer cells by TMZ along with Adhz60 is, at least in part, due to greater apoptosis induction within these cells.

TMZ enhances virotherapy by increasing virus replication in lung cancer but not in non-cancerous lung cells

Lung cancer cell lines were treated as described in the Figure 1. Three days after treatment, samples were collected and adenovirus production was determined via the TCID50 protocol using HEK293 cells. TMZ increased Adhz60 virus production approximately 100 fold in all three cancer cell lines tested compared to Adhz60-infected cells treated with the TMZ drug vehicle DMSO. Conversely, the production of Adwt viruses did not increase in the presence of TMZ compared with Adwt-infected cells in the presence of DMSO (Fig. 3A). Immunoblot analysis results showed that TMZ increased E1A expression by Adhz60, but TMZ treatment did not alter E1A expression via Adwt (Fig. 3B). This effect was probably caused by greater potency of Adwt in comparison with Adhz60; therefore, E1A expression reached its expression peak before TMZ could increase Adwt-mediated E1A expression.

Human lung non-cancerous MRC-5 cells were treated with the combined therapy or the respective controls. A crystal violet staining showed that Adhz60 alone did not induce CPE in MRC-5 cells. Most importantly, cells treated with Adhz60 + TMZ did not alter the induction of CPE in non-cancerous lung cells (Fig. 3C). In contrast, Adwt alone induced significant CPE in MRC5 non-cancerous lung cells (58% of cell viability) (Fig. 3D). Adwt-induced CPE was slightly increased in the presence of TMZ (52% of cell viability) (Fig. 3D). Additionally, a virus titration assay revealed that only Adwt-infected MRC-5 cells produced infective virus particles in MRC5 non-cancerous cells (Fig. 3E). Finally, E1A expression was dramatically lower in Adhz60-infected MRC5 non-cancerous cells; TMZ treatment did not increase E1A expression in these cells. Conversely, marked E1A expression was detected in Adwt-infected MRC5 non-cancerous cells; TMZ treatment slightly increased E1A expression by Adwt (Fig. 3F). These results suggest that TMZ does not increase Adhz60-mediated oncolysis in MRC5 non-cancerous lung cells.

TMZ induces autophagosome formation and accumulation of LC3-II in lung cancer cells

TMZ has been reported to induce autophagy in glioma cells (Lin et al., 2012). Therefore, the ability of TMZ to induce autophagy in lung cancer cells was evaluated. Lung cancer cells were transfected with pEGFP-LC3 and treated with DMSO or TMZ and then observed for the formation of cytoplasmic punctate GFP florescence. The conversion of cytoplasm-diffuse GFP-LC3-I to membrane-associated GFP-LC3-II forms punctate patterns, indicating LC3-II incorporation into the autophagosomes. This formation of punctate was observed at 48 h (Fig. 4A). TMZ induced significant GFP cellular puncta relative to DMSO-treated cells, which exhibited diffuse cytoplasmic GFP-florescence and very few punctate GFP expressing cells (8%). Among the lung cancer cell lines, A549 showed the greatest percentage of cells with GFP punctate pattern (57%), whereas Calu-1 and H441 had a lower percentage (48% and 51%, respectively). These results suggest that TMZ induces autophagy in lung cancer cells.

Next, the conversion of LC3-I to LC3-II, an autophagy maker (Kabeya et al., 2000), was evaluated. Immunoblot analysis revealed two reactive LC3 species: the upper band corresponding to LC3-I (19 kDa) and a lower band corresponding to LC3-II (17 kDa). Marked accumulation of LC3-II was observed in TMZ-treated cells at 48h and 72h, whereas no conversion was observed in DMSO-treated cells (Fig. 4B).

Combination of oncolytic adenovirus with temozolomide increases autophagy

Since TMZ and Adhz60 are known to induce autophagy separately (Lin et al., 2012; Rodriguez-Rocha et al., 2011), we investigated whether the combination of both treatments could induce greater autophagy than either treatment used alone. Lung cancer cells were treated with TMZ or Adhz60 alone at their respective IC_{50} or in combination; 72 h post-treatment, autophagy induction was evaluated by LC3-I to LC3-II conversion and by the decreased expression of p62, which is degraded during autophagy flux (Bjorkoy et al., 2005). Immunoblot analysis revealed a greater accumulation of LC3-II in Adhz60 + TMZtreated cells compared to either treatment alone in all cell lines tested (Fig. 4C). The decreased p62 expression was variable across these cancer cell lines (Fig. 4C). These results suggest that the combination of Adhz60 and TMZ induces greater autophagy in lung cancer cell lines than either treatment alone.

Autophagy inhibition partially protects lung cancer cells from combined therapy-mediated cell death

We assessed the cell killing effects of TMZ alone, Adhz60 alone, or in combination, in the presence of 3-MA (Rodriguez-Rocha et al., 2011) or Baf-A1 (Ulasov et al., 2009a) , which are two agents that inhibit autophagy by preventing the fusion of autophagosomes and lysosomes (Yamamoto et al., 1998). 3-MA inhibits autophagy during the formation of double-membrane structures, and Baf-A1 inhibits the maturation of autophagosomes when the cytosol is sequestered from the cytoplasm (Ravikumar et al., 2002). In our study, TMZ-induced toxicity increased in the presence of 3-MA, whereas, in presence of Baf-A1, cell viability was unchanged. The Adhz60-mediated cell death was significantly decreased by 3-MA and Baf-A1 treatments ($P < 0.05$) (Fig. 4D). Most importantly, the combined treatment of Adhz60 + TMZ was significantly impaired by the presence of 3-MA. This suggests that autophagy may play a role in the combined therapy- mediated cell death.

Oncolytic adenovirus lacking the entire E1B activates p-JNK

The adenovirus E1B gene products have been reported to strongly activate JNK (See and Shi, 1998), while TMZ was found to have induced autophagy through JNK activation in glioma cells (Lin et al., 2012). Because Adhz60 lacks the E1B gene, we hypothesized that TMZ-induced JNK activation could complement the lack of E1B-induced JNK activation, and virus replication would be enhanced. However, we found that Adhz60 activated JNK alone but TMZ did not in our experimental conditions. We hypothesized that Adhz60 could induce p-JNK expression via E1A; however, additional studies are necessary. The combination of both Adhz60 and TMZ appeared to result in a greater JNK activation at 48 h (Fig. 5). These results suggest that TMZ does not activate JNK in A549 lung cancer cells using these experimental conditions, and that TMZ-mediated JNK activation may not be

required to enhance Adhz60 replication and oncolysis in A549 cells. This result is consistent with the finding that the E1A-deleted Ad (dl312) displayed severely attenuated JNK activation, implicating the role of E1A as a p-JNK inducer (See and Shi, 1998).

Adhz60 downregulates MGMT expression in lung cancer cells

MGMT is highly expressed in human cancers and confers resistance to many clinically used alkylating agents such as TMZ (Srivenugopal et al., 2001). It was reported that overexpression of adenovirus E1A, which binds CBP/p300, strongly inhibited MGMT promoter activity (Bhakat and Mitra, 2000). Therefore, we explored the posibility that Adhz60 may decrease MGMT expression in lung cancer cells via E1A-mediated sequestion of p300, which promotes MGMT expression. Immunoblot analysis revealed that Adhz60 downregulated MGMT expression in all cancer cell lines; however, MGMT downregulation was greatest in A549 cells. The negative control AdLacZ did not affect MGMT expression (Fig. 6). These results suggest that, although Adhz60 was able to decrease MGMT expression, this effect might not be directly associated with the synergistic effect of Adhz60 and TMZ combined..

Efficient suppression of subcutaneous lung tumor growth in vivo by the combination of Adhz60 and TMZ

The combination of Adhz60 and TMZ was further assessed for its anti-tumor activity *in vivo* using a subcutaneous xenograft murine model and H441 lung cancer cells.. Mice bearing palpable tumors were randomized and underwent intratumoral injection of adenoviruses every three days for a total of four treatments; TMZ was administered via intraperitoneal injection. Representative tumors were harvested 24 hours after the final treatment following the euthanasia of mice. Tumor samples were then subjected to histopathological analysis to assess whether adenovirus hexon expression and apoptosis were possible mechanisms to induce tumor suppression. Immunohistochemical analysis revealed that hexon expression was detected in the Adhz60-treated group; however, hexon expression appeared to increase following treatment with the combination of Adhz60 and TMZ. Hexon was not detected in AdLacZ-, TMZ-, and AdLacZ + TMZ-treated groups. Detection of cleaved caspase-3-positive cells was observed in TMZ- and AdLacZ + TMZ-treated groups, whereas it was not detected in Adhz60 treated mice; however, a greater number of cleaved caspase-3-positive cells were observed in the tumors of mice treated with the combination of Adhz60 + TMZ (Fig. 7A).

Greater tumor suppression was observed with combined Adhz60 and TMZ treatment. Tumor sizes were approximately 41% smaller in Adhz60-treated mice and 12% in TMZ-treated group, whereas in Adhz60 + TMZ treatment group, tumor sizes were ~ 70% smaller compared to mice treated with the negative control virus AdLacZ (Fig. 7B). The final tumor volume was similar in the negative control and TMZ treatment groups. The differences in median tumor volumes at the conclusion of the experiment were statistically significant when comparing either treatment (TMZ or Adhz60) alone to mice treated in combination (Adhz60 + TMZ) (*$P < 0.05$). These results suggest that Adhz60 increases the sensitivity of lung cancer cells to TMZ, and that lung cancer tumor growth suppression by this therapeutic combination was, at least in part, mediated by increased caspase activation *in vivo*.

Discussion

TMZ has been reported to enhance oncolytic virotherapy in glioblastoma and melanoma cells (Jiang et al., 2015; Kaliberova et al., 2009). Additionally, oncolytic adenoviruses (OAds) have been shown to sensitize glioma cells to TMZ by repressing the DNA repair enzyme MGMT (Alonso et al., 2007). Other studies have reported that autophagy plays a key role in oncolytic virotherapy (Yokoyama et al., 2008), and that TMZ-induced autophagy enhances OAd replication (Ulasov et al., 2009b). These synergistic killing effects in glioblastoma were associated with the induction of both autophagy and apoptosis *in vitro* and *in vivo* (Jiang et al., 2013; Liikanen et al., 2013). Both reports found that virotherapy was enhanced, in part, due to increased virus replication. Therefore, we tested the ability of TMZ to enhance OAd virus replication in lung cancer cells known to be permissive or semi-permissive to Ad replication. It was found that the combination therapy of Adhz60 with TMZ has a synergistic killing effect in lung cancer cells (Figs. 1D and 1E). This enhanced anti-cancer efficacy may be explained by at least three possible mechanisms: increased apoptosis, virus replication, and autophagy. It was observed that TMZ did not further increase E1A expression in Adwt infected-cells (Fig. 3B). This effect was probably due to very high E1A expression by Adwt; therefore, Adwt may have reached its peak E1A expression before TMZ could increase Adwt-mediated E1A expression. Lower doses of Adwt or an early time point might be explored to observe the effect of TMZ in Adwt-infected cells.

More importantly, the combined therapy of Adhz60 and TMZ displayed minor cytotoxicity upon non-cancerous MRC5 lung cells. This suggests that the Adhz60-mediated killing effects were dependent upon E1B gene deletion, regardless of drug-induced autophagy. Therefore, the approach proposed here had limited toxicity in non-cancerous cells, suggesting a potentially favorable therapeutic index for this combination.

The precise mechanism by which TMZ enhances Adhz60-mediated oncolysis in lung cancer cells is not completely understood. However, it was found that TMZ initiated autophagy in lung cancer cells, and OAds may use TMZ-induced autophagy to increase viral replication (Figs. 3A and 3B). We previously reported that inhibition of autophagy with 3-methyladenine (3MA) resulted in a poor viral replication, while the induction of autophagy with rapamycin increased adenovirus yield (Rodriguez-Rocha et al., 2011). Herein, we found a similar effect when 3MA or Baf-A1 were used to inhibit the early and late phases of autophagy, respectively. This suggests that autophagy may play a role in the enhanced lung cancer cell death of these combined therapies. In fact, it was reported recently that the addition of 3-MA suppresses TMZ-induced autophagy and increases TMZ-induced apoptosis in glioma cells (Lin et al., 2012). This suggests TMZ induces a protective autophagy.

As a monotherapeutic, TMZ-induced autophagy appears to have a cytoprotective role. For example, TMZ can promote autophagy through the accumulation of reactive oxygen species (ROS), mitochondrial depolarization, and mitochondrial permeability transition pore (MPTP) opening to cause mitochondrial damage, resulting in protective autophagy (Lin et al., 2012). In this study, we examined whether TMZ could activate JNK in lung cancer cells.

However, we were unable to detect p-JNK in A549 lung cancer cells using these experimental conditions. Therefore, the precise mechanism by which TMZ induces autophagy in lung cancer cells remains unknown.

In summary, TMZ-induced autophagy provides a better cellular environment for adenovirus replication. The combination of both TMZ and Adhz60 enhances their potency reciprocally. This study represents a potential alternative to lung cancer therapy, because the increased oncolytic adenovirus replication induced by TMZ may facilitate the virus spread within the lung tumors.

Materials and Methods

Cell lines and culture conditions

Human embryonic kidney 293 (HEK-293) cells, human lung cancer permissive A549 & H1299 cells, semi-permissive H441 & Calu-1, and human lung non-cancerous fibroblast MRC-5 cell lines were purchased from the American Type Culture Collection (Rockville, MD). A549 and H1299 cells were grown in DMEM medium; H441was cultured in RPMI1640 medium; Calu-1 in McCoy's 5a medium; HEK-293 and WI-38 were grown in alpha-MEM medium. All media were supplemented as previously described (Egger et al., 2014). All cell culture reagents were obtained from Corning Cellgro.

Adenoviral vectors and drugs

A replication-deficient adenoviral vector AdLacZ expressing β-galactosidase under regulation of cytomegalovirus promoter was used as a control as previously described (Egger et al., 2014). The adenovirus serotype 5 wild type (Adwt) and a CRAd (Adhz60 *E1B*-deleted) were used as previously reported by us (Rao et al., 2004). TMZ and bafilomycin-A1 (Baf-A1) stock solutions of 100 mM and 1.6 mM, respectively, were prepared in dimethyl sulfoxide (DMSO) and stored at −20°C. 3-methyladenine (3-MA) was dissolved in H_2O at final concentration of 66 mM. All drugs were purchased from (Sigma-Aldrich, St Louis, MO).

Single and combined therapies

2.5×10^4 cells were plated in 24-well plates and treated 24 h later with indicated therapy. Viral infection was performed at an indicated multiplicity of infection (MOI) concentration, whereas TMZ treatment was performed at an indicated mM concentration. Cytopathic effect (CPE) was evaluated with crystal violet staining as described previously by our group (Cheng et al., 2015). Cell viability was assessed 72 h after experimental therapy by measuring the conversion the tetrazolium salt 3-(4,5-dimethylthiazol-2-yl)-2,5-diphenyltetrazolium (MTT) to formazan as described by our group (Egger et al., 2014). For control infection, we used cell line-specific media alone without virus or DMSO instead of TMZ. The IC_{50} for both virus and TMZ were determined. For combined therapies, cells were treated with Adhz60 and TMZ at their respective IC_{50} doses. For inhibitory studies, A549 cells were seeded as described above. The next day, either 3-MA (10 mM) (Rodriguez-Rocha et al., 2011; Ropolo et al., 2007) or BAF-A1 (10 nM) (Kanzawa et al., 2004) was added for further incubation. The drug containing media was removed and cells

were treated with Adhz60 at an MOI of 10 or TMZ at 0.75 mM, both for single and combined treatments. Seventy-two hours post-treatment, cell viability was evaluated by MTT assay as described above.

Analyses of combined effects of Adhz60 and TMZ

The additive effect refers to a combined effect of drugs that produces the sum of their individual effects. Synergism is the combined effect of drugs which is greater than the sum of individual effects. Antagonism is the combined effect of drugs which is less than the sum of individual effects (Chou, 2006; Wang et al., 2011). The combined effects of Adhz60 with TMZ on cell viability were analyzed with the median-effect methods of Chou and Talalay (Chou and Talalay, 1984) using CalcuSyn software (Biosoft, Ferguson, MO). The combination index (CI) values were used to evaluate the interaction between the virus and drug. For the fraction of virus affected combination index (Fa-CI) plot analysis, a $CI < 1$ is defined as synergism, a $CI = 1$ is defined as an additive effect, and a $CI > 1$ is defined as antagonism.

Annexin V staining and adenovirus titer analysis

Cells were stained with annexin V-PE and 7-AAD, according to the manufacturer's instructions (BD Pharmingen, San Diego CA). Cells were analyzed by FACScan flow cytometer (Becton Dickinson, Franklin Lakes, NJ) and with FlowJo software (Tree Star Inc., Ashland, OR). For titer analysis, cells were treated as described in the combined therapies. Seventy-two hours post-treatment, supernatants were collected. Adenoviruses released were titered by using a TCID50 end-point dilution method with HEK-293 cells seeded on 96-well plates as described previously (Rodriguez-Rocha et al., 2011).

Western blot analysis

Western blot analysis was performed using a standard procedure as described previously (Rodriguez-Rocha et al., 2011). The primary antibodies used were rabbit-antihuman cleaved caspase-3, SQSTM1/p62 (D5E2), phospho-SAPK/JNK (Thr183/Tyr185) (p-JNK) SAPK/JNK antibody total-JNK (t-JNK) (Cell Signaling, Danvers, MA), rabbit anti-LC3 polyclonal antibody (Sigma-Aldrich, St Louis, MO), mouse anti-adenovirus type 5 E1A (BD Pharmingen, San Diego CA), and rabbit-antihuman-actin (Sigma-Aldrich, St Louis, MO). The scanned band intensities were quantified using Gel-pro Analyzer 4.0 software (Media Cybernetics) according to the manufacturer's tutorial. Densitometric values for each band were expressed as integrated optical density (I.O.D.) and normalized to actin expression.

GFP-LC3 puncta

Plasmid vector containing green fluorescent protein (GFP) linked to microtubule-associated protein 1 light chain 3 (LC3) (Kabeya et al., 2000) was used to detect autophagosome formation in lung cancer cell lines. At 24-h post-transfection, cells were treated with DMSO or TMZ at its respective LD_{50} for each cell line. At 48h post-treatment, cells were examined under a fluorescence microscope. Cells were classified as having a predominantly diffuse GFP stain or having numerous punctate structures representing autophagosomes. Images were taken at 40× magnification with the EVOS FL Imaging System (Advanced Microscopy

Group) under 357/44 (nm) and 447/60 (nm) excitation and emission visualization. The percentage of cells with GFP puncta were calculated as the proportion of cells with GFP puncta divided by the total number of GFP expressing cells.

Mouse lung cancer xenograft model

Subcutaneous tumors were formed in the flanks of 6-week-old athymic BALB/c *nu/nu* male mice (Charles River Laboratories) by injecting 5×10^6 H441 human lung cancer cells in 100 μL of phosphate buffered saline (PBS). Seven days following injection, palpable tumors were formed. Treatment groups were as follows: AdLacZ, TMZ, AdLacZ + TMZ, Adhz60, and Adhz60 + TMZ. Mice were randomized and injected in the flank with Adhz60 (1×10^9 plaque forming units [pfu]) or Ad-LacZ (1×10^9 pfu) ($n = 6$ for each group) intratumorally every three days for a total of four treatments. TMZ was administered via intraperitoneal injections of 50 mg/kg (diluted in PBS) daily for five consecutive days. Tumor size was measured with calipers in two dimensions (length and width) every three days for 30 days, and tumor volume was estimated by the following equation:

$$V = \left(L \times W^2\right)/2$$

where V is volume, L is length and W is width. Animal experiments were performed in accordance with institutional guidelines and were approved by the University of Louisville Institutional Animal Care and Use Committee.

Immunohistochemistry

Tumors were excised 24h after the fourth injection following euthanization, fixed in 10% formalin, embedded in paraffin blocks, and processed for histological analysis. Expression of hexon and cleaved caspase-3 were evaluated. Mouse-antiadenovirus hexon protein (1:200) (Abcam, Cambridge, MA) or rabbit-antihuman cleaved caspase-3 (1:200) (Cell Signaling, Danvers, MA) Abs were used to detect hexon or cleaved caspase-3 expression, respectively. The slides were then washed with PBS, incubated with the standard ultra-Sensitive ABC peroxidase staining kit (PIERCE), and detected with diaminobenzidine tetrahydrochloride (DAB) solution containing 0.006% H_2O_2. Tissue sections stained without primary antibodies were used as negative controls. Photographs were taken with 20x magnification and analyzed with NIS-Elements BR 3.0 software (Nikon Instruments, Inc.).

Statistical analysis

One- and two-way ANOVA was used to determine differences in cell viability across different virus treatments and doses as appropriate. Statistically significant differences between control (AdLacZ) and active (Adhz60) virus therapy were determined by the significance of the interaction effect of dose and virus. Differences in cell viability across combination therapies were analyzed by one-way ANOVA. Post-hoc testing was performed with Tukey's adjustment to control for a significance level of 0.05. Tumor size differences between treatment groups were compared over the course of the experiment using repeated measures ANOVA. Tumor sizes at the conclusion of the experiment were compared using

one-way ANOVA, and post hoc testing of differences between groups were adjusted for multiple comparisons using Tukey's HSD.

Supplementary Material

Refer to Web version on PubMed Central for supplementary material.

Acknowledgments

This work was supported by Award Numbers GB120124 (JGGG) from Lung Cancer Research Foundation, R01CA129975 (H.S.Z.), and by grant R25-CA-134283 (J.N.) and (E.R.) from the National Cancer Institute. E.M.J. is recipient of a scholarship from the National Council of Science and Technology (CONACYT) of Mexico. We thank Margaret Abby for editing.

References

Alonso MM, Gomez-Manzano C, Bekele BN, Yung WK, Fueyo J. Adenovirus-based strategies overcome temozolomide resistance by silencing the O6-methylguanine-DNA methyltransferase promoter. Cancer Res. 2007; 67:11499–11504. [PubMed: 18089777]

Bhakat KK, Mitra S. Regulation of the human O(6)-methylguanine-DNA methyltransferase gene by transcriptional coactivators cAMP response element-binding protein-binding protein and p300. J Biol Chem. 2000; 275:34197–34204. [PubMed: 10942771]

Bjorkoy G, Lamark T, Brech A, Outzen H, Perander M, Overvatn A, Stenmark H, Johansen T. p62/SQSTM1 forms protein aggregates degraded by autophagy and has a protective effect on huntingtin-induced cell death. The Journal of cell biology. 2005; 171:603–614. [PubMed: 16286508]

Cheng PH, Rao XM, Duan X, Li XF, Egger ME, McMasters KM, Zhou HS. Virotherapy targeting cyclin E overexpression in tumors with adenovirus-enhanced cancer-selective promoter. J Mol Med (Berl). 2015; 93:211–223. [PubMed: 25376708]

Chou TC. Theoretical basis, experimental design, and computerized simulation of synergism and antagonism in drug combination studies. Pharmacological reviews. 2006; 58:621–681. [PubMed: 16968952]

Chou TC, Talalay P. Quantitative analysis of dose-effect relationships: the combined effects of multiple drugs or enzyme inhibitors. Advances in enzyme regulation. 1984; 22:27–55. [PubMed: 6382953]

Egger ME, McNally LR, Nitz J, McMasters KM, Gomez-Gutierrez JG. Adenovirus-Mediated FKHRL1/TM Sensitizes Melanoma Cells to Apoptosis Induced by Temozolomide. Human gene therapy. Clinical development. 2014; 25:186–195. [PubMed: 25238278]

Gozuacik D, Kimchi A. Autophagy and cell death. Curr Top Dev Biol. 2007; 78:217–245. [PubMed: 17338918]

Hay JG, Shapiro N, Sauthoff H, Heitner S, Phupakdi W, Rom WN. Targeting the replication of adenoviral gene therapy vectors to lung cancer cells: the importance of the adenoviral E1b-55kD gene. Hum Gene Ther. 1999; 10:579–590. [PubMed: 10094201]

Jiang G, Jiang AJ, Cheng Q, Tian H, Li LT, Zheng JN. A dual-regulated oncolytic adenovirus expressing interleukin-24 sensitizes melanoma cells to temozolomide via the induction of apoptosis. Tumour biology : the journal of the International Society for Oncodevelopmental Biology and Medicine. 2013; 34:1263–1271. [PubMed: 23430584]

Jiang G, Sun C, Li RH, Wei ZP, Zheng JN, Liu YQ. Enhanced antitumor efficacy of a novel oncolytic adenovirus combined with temozolomide in the treatment of melanoma in vivo. Journal of cancer research and clinical oncology. 2015; 141:75–85. [PubMed: 25103017]

Kabeya Y, Mizushima N, Ueno T, Yamamoto A, Kirisako T, Noda T, Kominami E, Ohsumi Y, Yoshimori T. LC3, a mammalian homologue of yeast Apg8p, is localized in autophagosome membranes after processing. The EMBO journal. 2000; 19:5720–5728. [PubMed: 11060023]

Kaliberova LN, Krendelchtchikova V, Harmon DK, Stockard CR, Petersen AS, Markert JM, Gillespie GY, Grizzle WE, Buchsbaum DJ, Kaliberov SA. CRAdRGDflt-IL24 virotherapy in combination with chemotherapy of experimental glioma. Cancer Gene Ther. 2009; 16:794–805. [PubMed: 19363468]

Kanzawa T, Germano IM, Komata T, Ito H, Kondo Y, Kondo S. Role of autophagy in temozolomide-induced cytotoxicity for malignant glioma cells. Cell death and differentiation. 2004; 11:448–457. [PubMed: 14713959]

Liikanen I, Ahtiainen L, Hirvinen ML, Bramante S, Cerullo V, Nokisalmi P, Hemminki O, Diaconu I, Pesonen S, Koski A, Kangasniemi L, Pesonen SK, Oksanen M, Laasonen L, Partanen K, Joensuu T, Zhao F, Kanerva A, Hemminki A. Oncolytic adenovirus with temozolomide induces autophagy and antitumor immune responses in cancer patients. Mol Ther. 2013; 21:1212–1223. [PubMed: 23546299]

Lin CJ, Lee CC, Shih YL, Lin CH, Wang SH, Chen TH, Shih CM. Inhibition of mitochondria- and endoplasmic reticulum stress-mediated autophagy augments temozolomide-induced apoptosis in glioma cells. PloS one. 2012; 7:e38706. [PubMed: 22745676]

Mattern J, Koomagi R, Volm M. Smoking-related increase of O6-methylguanine-DNA methyltransferase expression in human lung carcinomas. Carcinogenesis. 1998; 19:1247–1250. [PubMed: 9683184]

Murray CJ, Lopez AD. Measuring the global burden of disease. N Engl J Med. 2013; 369:448–457. [PubMed: 23902484]

Newman RA, Kondo Y, Yokoyama T, Dixon S, Cartwright C, Chan D, Johansen M, Yang P. Autophagic cell death of human pancreatic tumor cells mediated by oleandrin, a lipid-soluble cardiac glycoside. Integr Cancer Ther. 2007; 6:354–364. [PubMed: 18048883]

Rao XM, Tseng MT, Zheng X, Dong Y, Jamshidi-Parsian A, Thompson TC, Brenner MK, McMasters KM, Zhou HS. E1A-induced apoptosis does not prevent replication of adenoviruses with deletion of E1b in majority of infected cancer cells. Cancer Gene Ther. 2004; 11:585–593. [PubMed: 15338010]

Ravikumar B, Duden R, Rubinsztein DC. Aggregate-prone proteins with polyglutamine and polyalanine expansions are degraded by autophagy. Human molecular genetics. 2002; 11:1107–1117. [PubMed: 11978769]

Rodriguez-Rocha H, Gomez-Gutierrez JG, Garcia-Garcia A, Rao XM, Chen L, McMasters KM, Zhou HS. Adenoviruses induce autophagy to promote virus replication and oncolysis. Virology. 2011; 416:9–15. [PubMed: 21575980]

Ropolo A, Grasso D, Pardo R, Sacchetti ML, Archange C, Lo Re A, Seux M, Nowak J, Gonzalez CD, Iovanna JL, Vaccaro MI. The pancreatitis-induced vacuole membrane protein 1 triggers autophagy in mammalian cells. J Biol Chem. 2007; 282:37124–37133. [PubMed: 17940279]

See RH, Shi Y. Adenovirus E1B 19,000-molecular-weight protein activates c-Jun N-terminal kinase and c-Jun-mediated transcription. Molecular and cellular biology. 1998; 18:4012–4022. [PubMed: 9632786]

Srivenugopal KS, Shou J, Mullapudi SR, Lang FF Jr. Rao JS, Ali-Osman F. Enforced expression of wild-type p53 curtails the transcription of the O(6)-methylguanine-DNA methyltransferase gene in human tumor cells and enhances their sensitivity to alkylating agents. Clinical cancer research : an official journal of the American Association for Cancer Research. 2001; 7:1398–1409. [PubMed: 11350911]

Tatar Z, Thivat E, Planchat E, Gimbergues P, Gadea E, Abrial C, Durando X. Temozolomide and unusual indications: review of literature. Cancer Treat Rev. 2013; 39:125–135. [PubMed: 22818211]

Tyler MA, Ulasov IV, Lesniak MS. Cancer cell death by design: apoptosis, autophagy and glioma virotherapy. Autophagy. 2009; 5:856–857. [PubMed: 19430207]

Ulasov IV, Sonabend AM, Nandi S, Khramtsov A, Han Y, Lesniak MS. Combination of adenoviral virotherapy and temozolomide chemotherapy eradicates malignant glioma through autophagic and apoptotic cell death in vivo. Br J Cancer. 2009a; 100:1154–1164. [PubMed: 19277041]

Ulasov IV, Tyler MA, Zhu ZB, Han Y, He TC, Lesniak MS. Oncolytic adenoviral vectors which employ the survivin promoter induce glioma oncolysis via a process of beclin-dependent autophagy. International journal of oncology. 2009b; 34:729–742. [PubMed: 19212678]

Wang S, Meckling KA, Marcone MF, Kakuda Y, Tsao R. Synergistic, additive, and antagonistic effects of food mixtures on total antioxidant capacities. Journal of agricultural and food chemistry. 2011; 59:960–968. [PubMed: 21222468]

Yamamoto A, Tagawa Y, Yoshimori T, Moriyama Y, Masaki R, Tashiro Y. Bafilomycin A1 prevents maturation of autophagic vacuoles by inhibiting fusion between autophagosomes and lysosomes in rat hepatoma cell line, H-4-II-E cells. Cell structure and function. 1998; 23:33–42. [PubMed: 9639028]

Yokoyama T, Iwado E, Kondo Y, Aoki H, Hayashi Y, Georgescu MM, Sawaya R, Hess KR, Mills GB, Kawamura H, Hashimoto Y, Urata Y, Fujiwara T, Kondo S. Autophagy-inducing agents augment the antitumor effect of telerase-selve oncolytic adenovirus OBP-405 on glioblastoma cells. Gene Ther. 2008; 15:1233–1239. [PubMed: 18580968]

Zhang XD, Wu JJ, Gillespie S, Borrow J, Hersey P. Human melanoma cells selected for resistance to apoptosis by prolonged exposure to tumor necrosis factor-related apoptosis-inducing ligand are more vulnerable to necrotic cell death induced by cisplatin. Clinical cancer research : an official journal of the American Association for Cancer Research. 2006; 12:1355–1364. [PubMed: 16489094]

Highlights

- TMZ enhances virotherapy in three lung cancer cell lines
- Oncolytic adenovirus does not lose its cancer selectivity upon TMZ treatment
- Combined therapy of Adhz60 and TMZ has synergistic killing effect in vitro

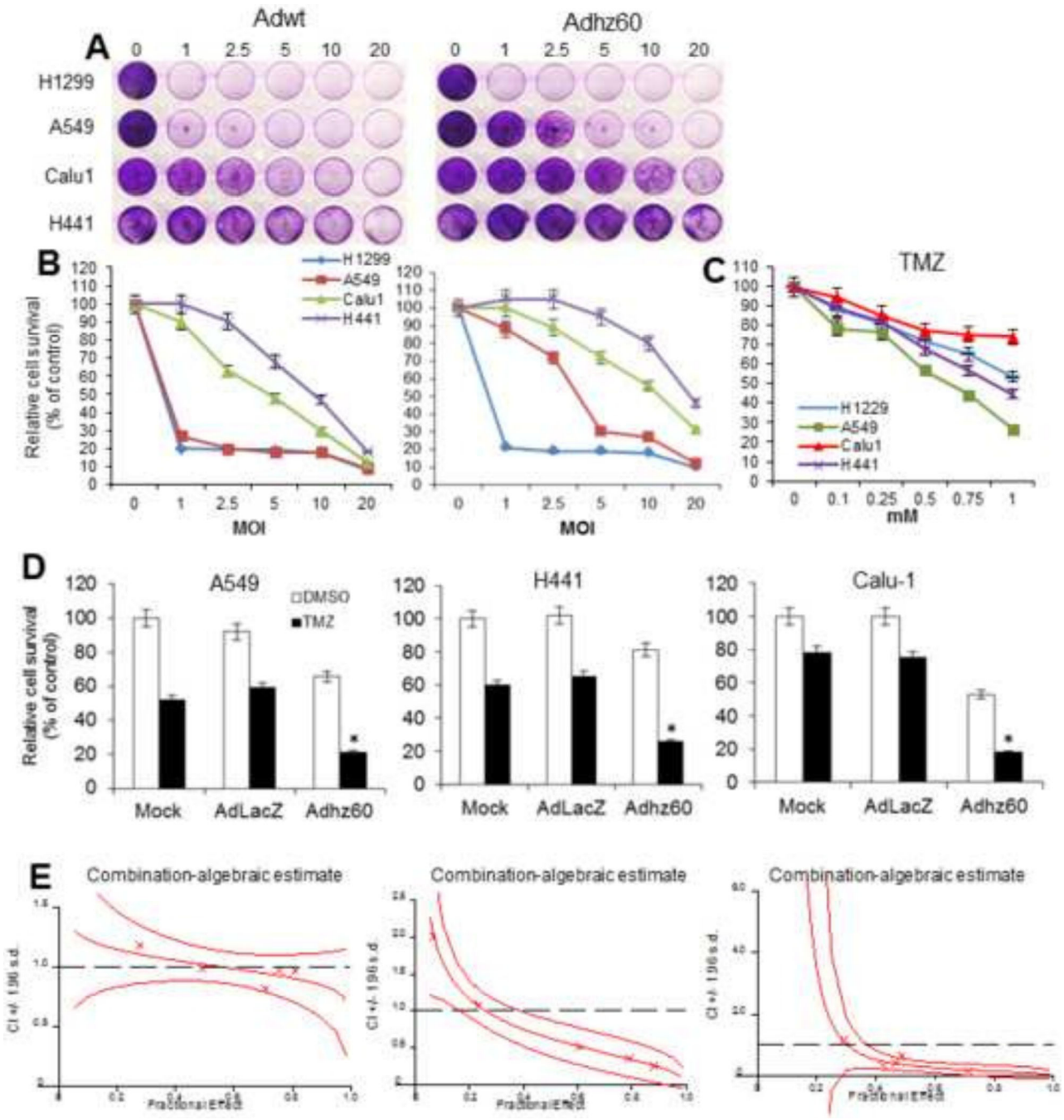

Figure 1. Evaluation of oncolytic adenovirus-mediated cytopathic effect in permissive and non-permissive lung cancer cells and determination of temozolomide half maximal inhibitory concentration (IC_{50})

(A) Permissive H1299 and A549 or semi-permissive Calu1 and H441 lung cancer cell lines were infected with Adwt or Adhz60 at a multiplicity of infection (MOI) concentration of 0, 1, 2.5, 5, 10, and 20. At 72h post-infection, crystal violet staining was used to evaluate cytopathic effect. A representative staining is shown of three experiments performed. ***(B)*** Cell viability was calculated by measuring the absorbance of solubilized dye at 590 nm. Each point represents the mean of three independent experiments ± standard deviation (SD;

bars). ***(C)*** The cell lines above-mentioned were treated with temozolomide (TMZ) at concentratons of 0, 0.1, 0.25, 0.5, 0.75, and 1 mM. A MTT assay was used to determine cell survival at 72h post-treatment. Each point represents the mean of three independent experiments ± standard deviation (SD; *bars*). ***(D)*** Human lung cancer cell lines were treated with Adhz60 and TMZ at the following doses for Adhz60 and TMZ, respectively: A549 (2.5 MOI, 0.6 mM), Calu1 (10 MOI, 1 mM), and H441 (20 MOI, 0.75 mM). AdLacZ was used at 10 MOI for all cell lines. DMSO was added as a control at its respective volume for each cell line. Cytotoxic effect was evaluated as described in (A). Results represent the mean of three repeated measurements ± standard deviation (SD; *error bars*) (*$p<0.05$ for all cell lines). ***(E)*** The quantitated cell viability data were analyzed by CalcuSyn software. The X-marks represent the combination index (CI) values of the combination treatment groups. The middle curve line represents the simulated combination index values of the combination treatment groups surrounded by two lines of algebraic estimations of the 95% Confidence Intervals.

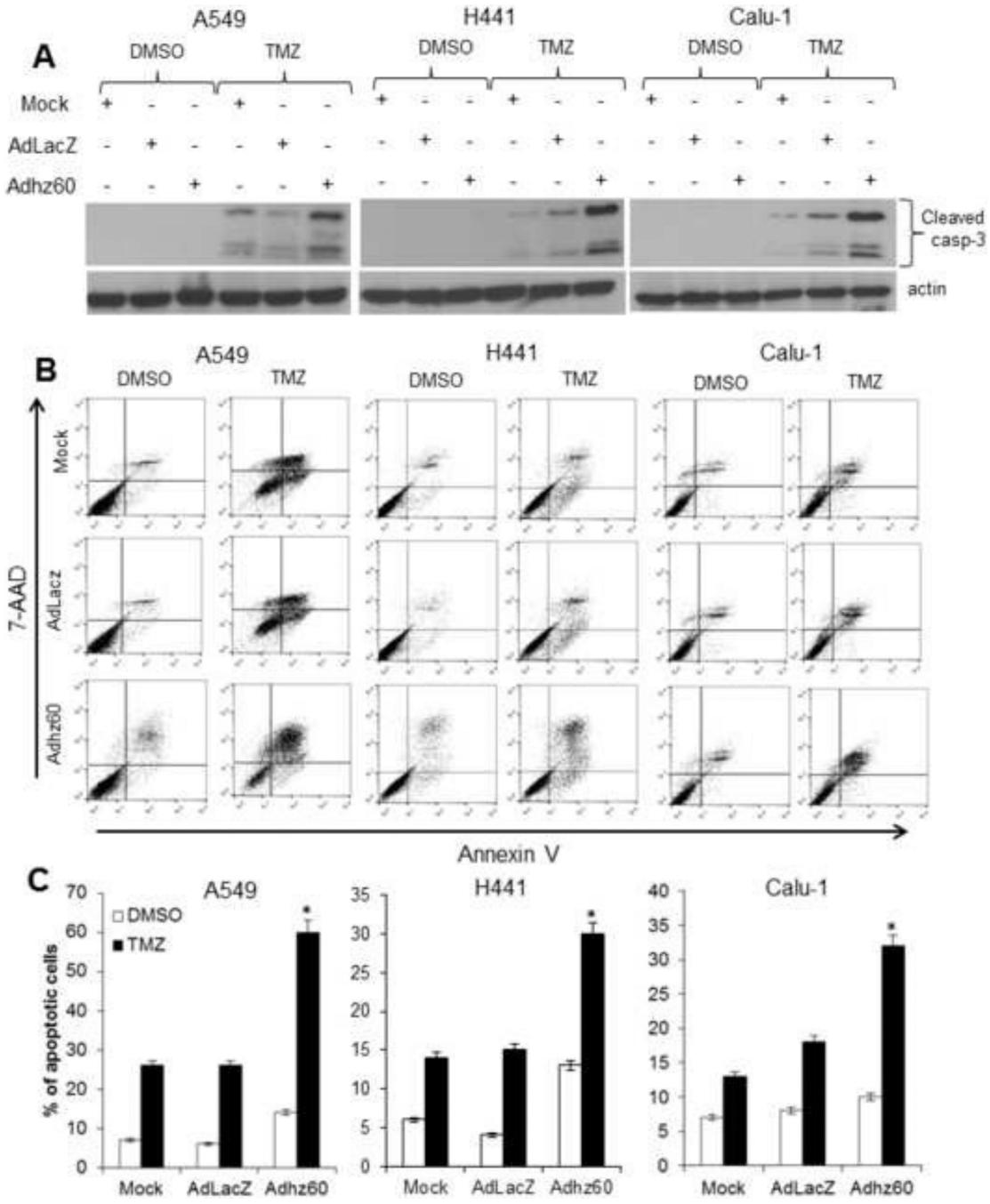

Figure 2. Evaluation of apoptosis induction

Whole cell protein lysates were collected 72h after indicated treatment (mock, AdLacZ +TMZ, Adhz60+TMZ). ***(A)*** Expression of cleaved caspase-3 was detected. ***(B)*** A549, H441, and Calu1 lung cancer cells were stained with annexin V-PE and 7-aminoactinomycin D (7-AAD). Positive cells for annexin V-PE and 7-AAD staining were analyzed by FACScan flow cytometer with FlowJo software. ***(C)*** Results represent the mean of three independent experiments ± standard deviation (SD; *error bars*) (*$P < 0.05$).

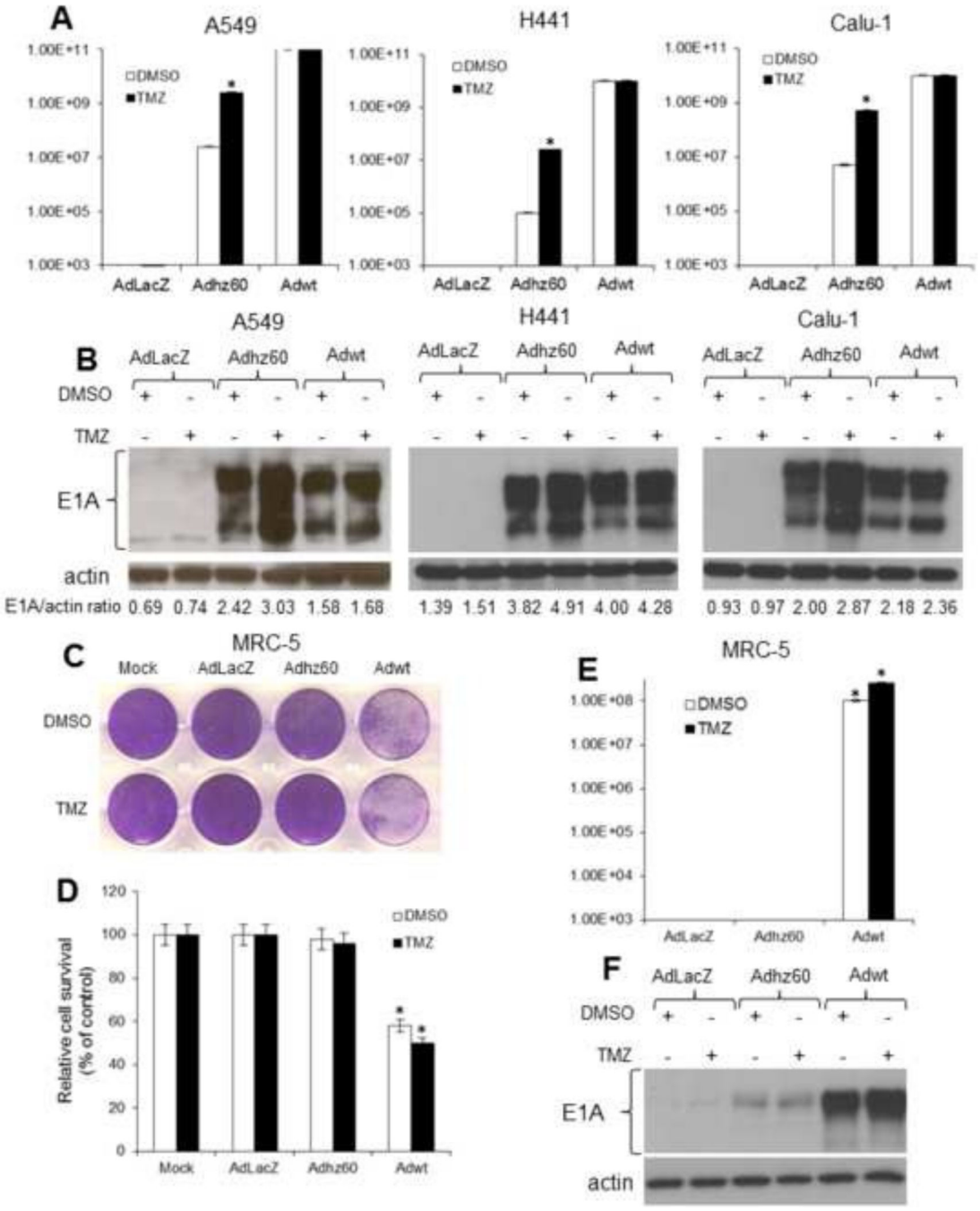

Figure 3. Effect of temozolomide (TMZ) on oncolytic adenovirus replication in permissive, non-permissive, and lung non-cancerous cells

(A) Lung cancer cells were treated as described in Figure 1. Seventy-two hours post-treatment, supernatants were collected and used to determine adenovirus yield from each cell line. Results represent the mean of three independent experiments ± standard deviation (SD; *error bars*) (**P* < 0.05). ***(B)*** Whole cell protein lysates were collected at 72h following indicated treatment. Expression of adenovirus E1A was detected by Western blot analysis. The values indicate the ratios of normalized band intensities of E1A expression profiles to actin. *(C)* MRC-5 cells were not infected (mock) or infected at a multiplicity of infection

(MOI) concentration of 5 with AdLacZ, Adhz60, or Adwt followed by DMSO (6 μl) or 0.6 mM of TMZ. ***(D)*** Seventy-two hours post–treatment, cell viability was calculated by measuring the absorbance of solubilized dye at 590 nm. Each point represents the mean of three independent experiments ± standard deviation (SD; *bars*). ***(E)*** Release of infectious virus particles was determined as described in (A). Results represent the mean of three independent experiments ± standard deviation (SD; *error bars*) (*$P < 0.05$). ***(F)*** Expression of adenovirus E1A was detected by Western blot analysis.

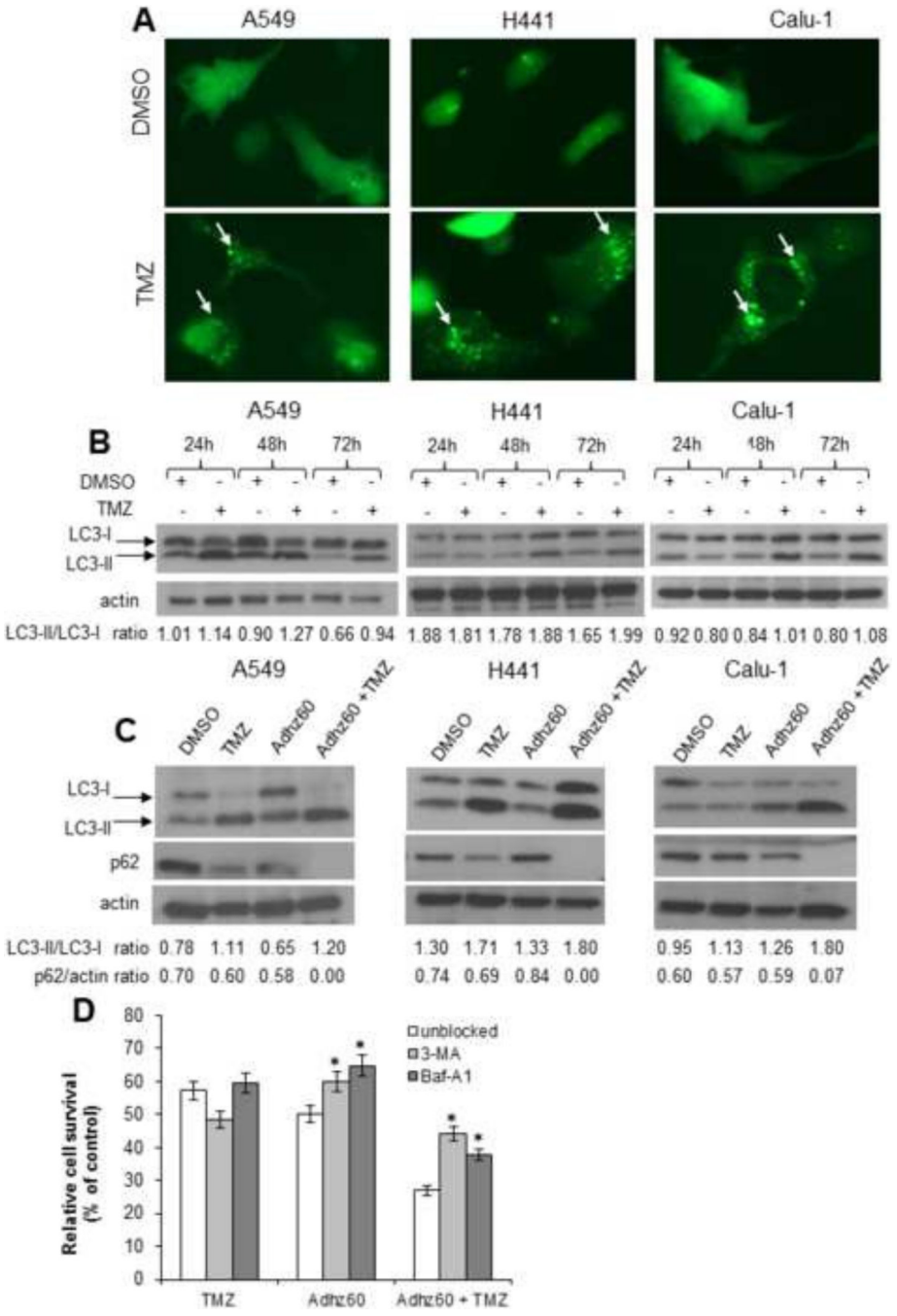

Figure 4. Evaluation of temozolomide (TMZ) ability to induce autophagy in lung cancer cells, enhanced autophagy using combination therapy, and the effect of autophagy inhibition using combined therapy-mediated cytotoxicity

(A) Lung cancer cells were transfected with pEGFP-LC3 followed by DMSO (A549: 6 μl; H441: 7.5 μl; and Calu1: 10 μl) or TMZ (A549: 0.6 mM; H441: 0.75 mM; Calu1: 1 mM) treatments. Integration of GFP-LC3 into the autophagosome is depicted by punctate structures and was analyzed by fluorescence microscopy at 48h post-treatment. Images were taken at 40× magnification with the EVOS FL Imaging System (Advanced Microscopy Group) under 357/44 (nm) and 447/60 (nm) excitation and emission visualization. The

percentage of cells with GFP punctuate pattern was calculated as punctuate GFP cell per total GFP cell %. A representative experiment showing punctuation (arrows) is shown from three performed. ***(B)*** LC3 expression and modification were analyzed in a time course assay. ***(C)*** Human lung cancer cell lines were treated with Adhz60 and TMZ alone or in combination at the following doses for Adhz60 and temozolomide (TMZ), respectively: A549 (2.5 MOI, 0.6 mM), Calu1 (10 MOI, 1 mM), and H441 (10 MOI, 0.75 mM). DMSO was added as a control at its respective volume for each cell line. Expression of LC3-I, LC3-II, and p62 were evaluated by Western blotting. Actin was used as a loading control. The values indicate the ratios of normalized band intensities of LC3I and LC3II or p62 expression profiles to actin. A representative experiment is shown. ***(D)*** A549 cells were cultured in the presence or absence of either 3-MA (10 mM) or BAF-A1 (10 nM). Media containing the drug was removed the next day, and the cells were treated with Adhz60 at a multiplicity of infection (MOI) concentration of 10 or TMZ at 0.75 mM, both for single and combined treatments. Seventy-two hours post-treatment, cell viability was evaluated by MTT assay. Results represent the mean of three independent experiments ± standard deviation (SD; *error bars*) (*$P < 0.05$).

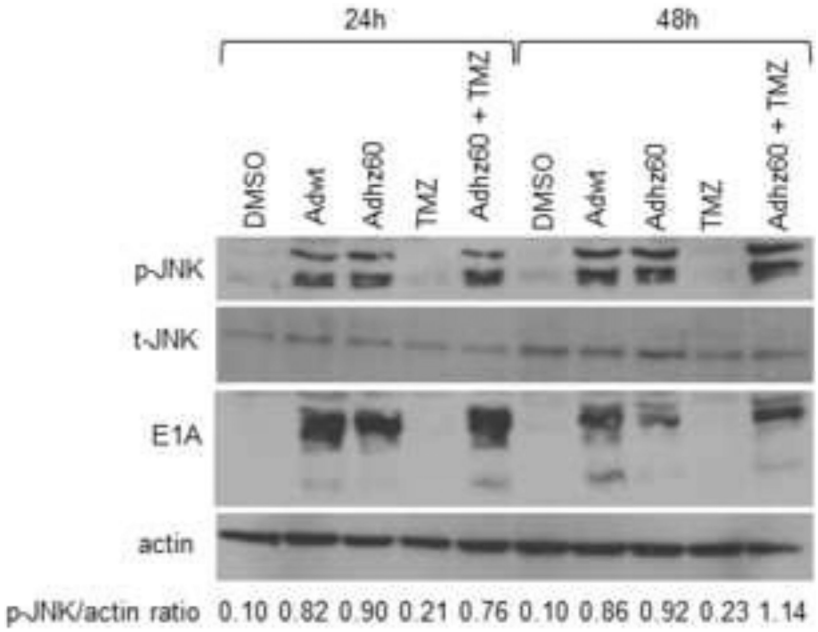

Figure 5. Evaluation of p-JNK, t-JNK, and E1A expressions in the combination therapy

A549 human lung cancer cells were infected at a multiplicity of infection (MOI) concentration of 2.5 alone or in combination with temozolomide (TMZ) at a 0.6 mM concentration. Expression of p-JNK, t-JNK, E1A, and actin were evaluated at 24h and 48h post-treatment by Western blot analysis. Actin was used as a loading control. These values indicate the ratios of normalized band intensities of p-JNK to actin expression. One representative experiment is shown.

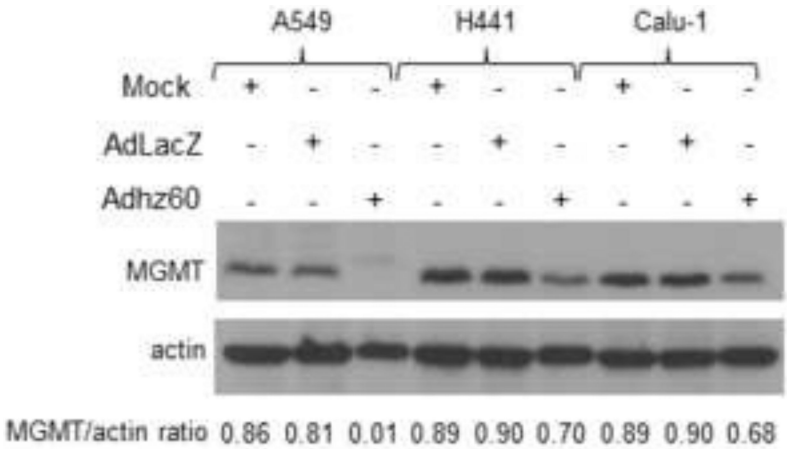

Figure 6. Assessment of MGMT expression

Human lung cancer cell lines were not infected (mock) or infected with AdLacZ at a multiplicity of infection (MOI) concentration of 10 for all cell lines or Adhz60 at the following doses: A549 (2.5 MOI), H441 (20 MOI), and Calu1 (10 MOI). Whole cell protein lysates were collected 72h after treatment. MGMT was detected by Western blot analysis. Actin was used as a loading control. These values indicate the ratios of normalized band intensities of MGMT to actin expression. One representative experiment from three is shown.

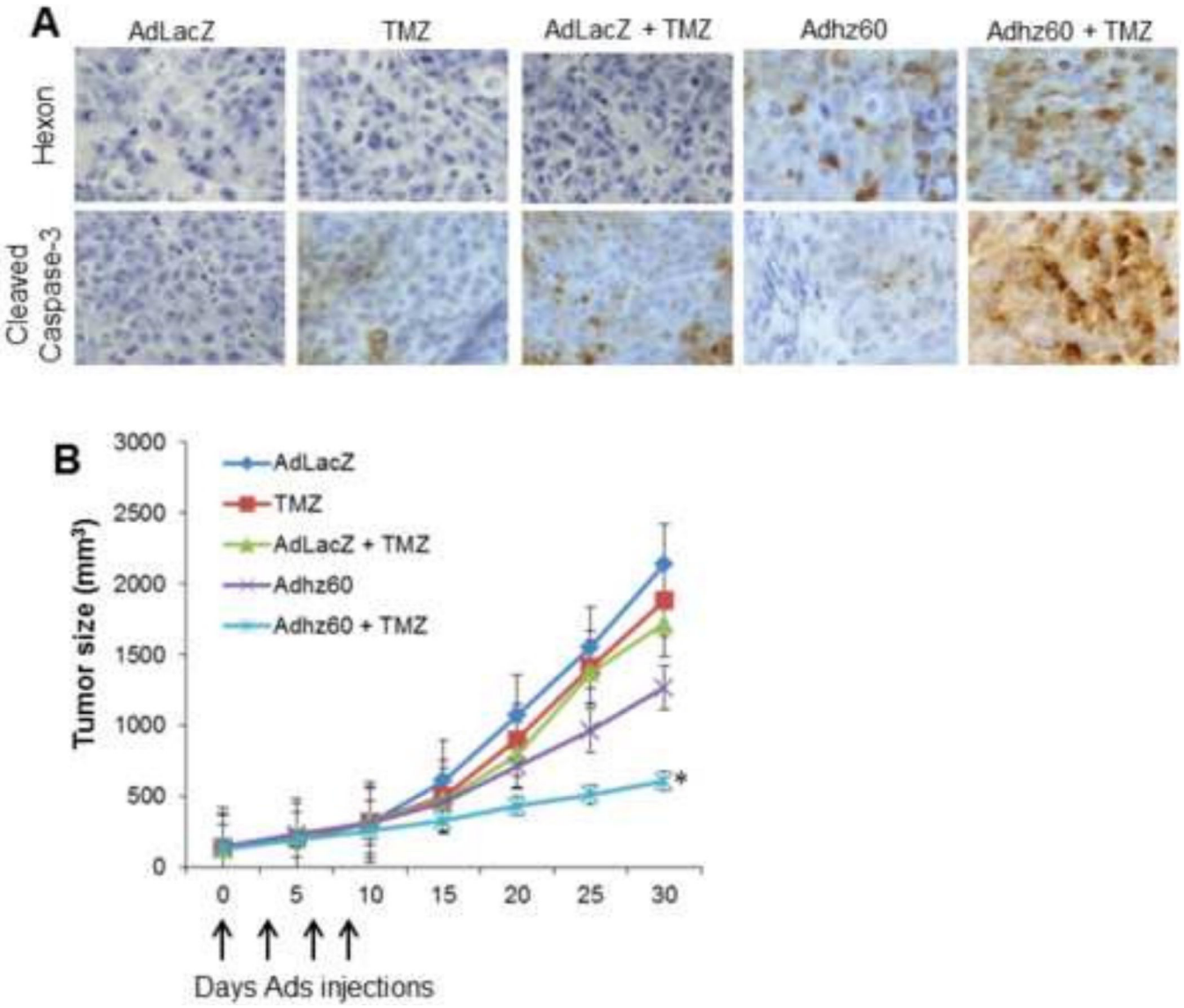

Figure 7. Evaluation of the therapeutic potential of combined therapy of Adhz60 with temozolomide in subcutaneous lung cancer mouse model

Flank lung cancer xenografts were developed by injection of H441 human lung cancer cells subcutaneously. Therapy was initiated 7 days after tumor injection when palpable tumors were formed. Treatments (*n*=6) were as follows: Ad-LacZ (control), Adhz60, temozolomide (TMZ), AdLacZ + TMZ, and Adhz60 + TMZ. Virus therapy was delivered by intratumoral injection every 3 days for a total of 4 doses (vertical arrows). TMZ was administered by intraperitoneal injection daily for 5 days. Tumor volume (V) was plotted against time and was determined by the equation $V = (L \times W^2)/2$, where L is the length and W is the width of the tumor. ***(A)*** Immunohistochemistry of excised tumor samples with hexon and cleaved caspase-3 indicate increased hexon expression and apoptosis activation with combined treatment of Adhz60 and TMZ (Adhz60 + TMZ). ***(B)*** Shows mean tumor volumes over the 30-day experiment estimated by caliper measurements every 5 days. Tumor size differences between treatment groups were compared over the course of the experiment using repeated

measures ANOVA. Tumor sizes at the conclusion of the experiment were compared using one-way ANOVA, and post hoc testing of differences between groups was adjusted for multiple comparisons using Tukey's HSD. Tumor size in the Adhz60 + TMZ treatment group had significantly decreased (SD; *error bars*) (*$P < 0.05$).